Analysis and control of optimal power distribution for multi-objective wireless charging systems

Zhang, Zhen; Tong, Ruilin; Liang, Zhenyan; Liu, Chunhua; Wang, Jiang

Published in:
Energies

Published: 01/07/2018

Published version (DOI):
10.3390/en11071726

Publication details:
Zhang, Z., Tong, R., Liang, Z., Liu, C., & Wang, J. (2018). Analysis and control of optimal power distribution for multi-objective wireless charging systems. *Energies*, *11*(7), Article 1726. https://doi.org/10.3390/en11071726

energies

MDPI

Article

Analysis and Control of Optimal Power Distribution for Multi-Objective Wireless Charging Systems

Zhen Zhang [1], Ruilin Tong [1], Zhenyan Liang [1], Chunhua Liu [2,*] and Jiang Wang [1]

[1] School of Electrical and Information Engineering, Tianjin University, Tianjin 300072, China; zhangz@tju.edu.cn (Z.Z.); tongrl@tju.edu.cn (R.T.); liangzy@outlook.com (Z.L.); jiangwang@tju.edu.cn (J.W.)
[2] School of Energy and Environment, City University of Hong Kong, Hong Kong, China
* Correspondence: chunliu@cityu.edu.hk

Received: 15 June 2018; Accepted: 27 June 2018; Published: 2 July 2018

Abstract: This paper proposes an optimal power distribution method for multi-objective wireless power transfer (WPT) systems, aiming to improve the transmission flexibility and satisfy various power demands. Previous studies have barely explored the impact of wide-range and unpredictable variations of load parameters on the performance of multi-channel power transmissions. In this paper, by taking the impact of equivalent impedance, motion, power demand variation and response speed of charging object into consideration, an optimal power distribution scheme with fast response, high stability and high accuracy is proposed to satisfy various power demands from multiple objectives including portable electronics, moving electric vehicles (EVs), batteries and super capacitors, without using any communication networks. The effectiveness of the proposed control scheme is demonstrated by simulation results based on different charging cases and experimental results based on a 10 W prototype.

Keywords: contactless charging; electric vehicle (EV); wireless power transfer (WPT)

1. Introduction

Recently, wireless power transfer (WPT) provides a brand new method for power transmission with salient advantages of cordless energization, multiple-channel transmission and flexibility by comparing with the traditional charging way. In particular, the inductive power transfer (IPT) utilizes the induced electromagnetic field to make the energy receptor harness the power over the air [1–4], which has been widely adopted for various applications, such as portable consumer electronics [5], implantable devices [6,7] etc.

Electric vehicle (EV), which has higher efficiency and higher stability, is getting increasing attention [8,9]. In Reference [10], a gearless motor with smoother torque and better torque density for EV is analyzed and designed, which makes EV driving more viable. In Reference [11], electromagnetic compatibility on charging EV is discussed and well concerned, which secures the charging procedure. The combination of EV and WPT combine the advantages of both EV and WPT, and further eliminate the limitation of battery energy storage and charging [12,13].

As one of its salient advantages, the power can be transmitted to multiple objectives wirelessly and simultaneously [14,15]; problems of cable entanglement, cable corrosion and number of charging ports are eliminated, which greatly improves charging flexibility and reduces system cost. In multi-objective conditions, however, the fairness of power distribution should be taken into account according to various power demands of loads. In previous studies, a circuit model was proposed for the design procedure of WPT systems and the analysis of the transmission efficiency [16–18]. In Reference [19], a maximum power transfer method for WPT systems was proposed to ensure the maximum power transmission. In order to optimize the efficiency for multi-objective transmission, a selective WPT

system was proposed by changing the excitation frequency [20,21]. Since the accurate resonant frequency is required for multiple receivers, the presented scheme should take into account the wide-range and unpredictable variation of receptor parameters in practical applications, which inevitably deteriorates the implementability. In Reference [22], an optimal power distribution can be achieved by choosing loads' resistance, but the value of resistance is calculated based on the coupling rate and coil inductance, while in public applications, coupling rate and coil inductance varies unpredictably, which causes this calculation to be infeasible.

Previous studies cannot deal with the uncertainties of the receptor number, load impedance, power consumption and load adjustment for the power distribution, which inevitably deteriorates the transmission performance of the multi-objective WPT systems. Accordingly, this paper proposes an impedance adjustment method independent of the communication, which can effectively achieve an optimal power distribution among static, moving, constant power demand and inconstant power demand objects with fast response, high stability and high accuracy. Furthermore, the proposed method can be taken into application on charging portable electronics, implantable devices and EVs. This paper is organized as follows. Mathematic model is analyzed in Section 2. Power distribution considerations are analyzed firstly in Section 3, based on the analysis, a control scheme for optimal power distribution is proposed. Section 4 verifies the proposed control scheme. Section 5 concludes this paper.

2. Mathematic Model

In multi-objective WPT systems, the flux equation of one excitation coil and multiple receptor coil can be expressed as:

$$\begin{cases} \psi_{ex} = L_{ex} i_{ex} + \sum M_{rei} i_{rei} \\ \psi_{rei} = L_{rei} i_{rei} + M_{rei} i_{ex} \end{cases}, \tag{1}$$

where ψ_{ex} represents the flux linkage of the excitation coil, ψ_{rei} represents the flux linkage of the ith receptor coil, L_{ex} represents the self-inductance of the excitation coil, L_{rei} represents the self-inductance of the ith receptor coil and M_{rei} represents the mutual inductance between the excitation coil and the ith receptor. The "ex" in the subscript means "excitation" and the "re" in the subscript means "receptor". The "i" in the subscript means the index of the receptor. To achieve maximum current, there should be capacitors to match reactive impedance in excitation and receptor circuits. The voltage equation of the excitation circuit and the receptor circuit can be expressed as:

$$\begin{cases} u_{ex} = r_{ex} i_{ex} + \frac{d\psi_{ex}}{dt} + \frac{1}{C_{ex}} \int i_{ex} dt \\ u_{rei} = r_{rei} i_{rei} + \frac{d\psi_{rei}}{dt} + \frac{1}{C_{rei}} \int i_{rei} dt \end{cases}, \tag{2}$$

where u_{ex}, r_{ex}, i_{ex} and u_{rei}, r_{rei}, i_{rei} are voltage, resistance, current of excitation circuit and the ith receptor, respectively. By substituting (1) into (2), it yields:

$$\begin{cases} u_{ex} = r_{ex} i_{ex} + L_{ex} \frac{di_{ex}}{dt} + \sum M_{rei} \frac{di_{rei}}{dt} + \frac{1}{C_{ex}} \int i_{ex} dt \\ u_{rei} = r_{rei} i_{rei} + L_{rei} \frac{di_{rei}}{dt} + M_{rei} \frac{di_{ex}}{dt} + \frac{1}{C_{rei}} \int i_{rei} dt \end{cases}. \tag{3}$$

In WPT systems, the supply voltage of the excitation circuit is a sinusoidal wave. Besides, in the excitation and receptor circuit, the inductor and capacitor connect in series. The current gain of the excitation and receptor circuit in frequency domain can be calculated as:

$$\begin{cases} G_{ex}(\omega) = \frac{j\omega C_{ex}}{1 + j\omega r_{ex} C_{ex} - \omega^2 L_{ex} C_{ex}} \\ G_{rei}(\omega) = \frac{j\omega C_{rei}}{1 + j\omega r_{rei} C_{rei} - \omega^2 L_{rei} C_{rei}} \end{cases}, \tag{4}$$

where G_{ex} and G_{rei} mean the current of the excitation and receptor circuit, respectively. ω means the

working angular frequency. When the circuits work in resonance mode, namely:

$$\begin{cases} \omega_0 = \frac{1}{\sqrt{L_{ex}C_{ex}}} \\ \omega_0 = \frac{1}{\sqrt{L_{rei}C_{rei}}} \end{cases}. \tag{5}$$

G_{ex} and G_{rei} can meet the maximum value. The resonance frequency ω_0 is selected as the working frequency for the WPT system. Besides, the receptors are usually passive, namely u_{rei} equals 0. Therefore, the circuit equation can be transformed to the symbolic-complex model as:

$$\begin{cases} \dot{u}_{ex} = r_{ex}\dot{i}_{ex} + j\omega_0 L_{ex}\dot{i}_{ex} + j\omega_0 \sum M_{rei}\dot{i}_{rei} - \frac{j}{\omega_0 C_{ex}}\dot{i}_{ex} \\ 0 = r_{rei}\dot{i}_{rei} + j\omega_0 L_{rei}\dot{i}_{rei} + j\omega_0 M_{rei}\dot{i}_{ex} - \frac{j}{\omega_0 C_{rei}}\dot{i}_{rei} \end{cases}. \tag{6}$$

Then, the current of the excitation and receptor circuits can be obtained as:

$$\begin{cases} \dot{i}_{ex} = \frac{\dot{u}_{ex}}{r_{ex} + j\omega_0 L_{ex} - \frac{j}{\omega C_{ex}} + j\omega_0 \sum \frac{\omega_0^2 C_{rei} M_{rei}^2}{1 + j\omega_0 C_{rei} r_{rei} - \omega_0^2 L_{rei} C_{rei}}} \\ \dot{i}_{rei} = \frac{\omega_0^2 C_{rei} M_{rei}}{1 + j\omega_0 C_{rei} r_{rei} - \omega_0^2 C_{rei} L_{rei}}\dot{i}_{ex} \end{cases}. \tag{7}$$

Since the reactive impedance can be eliminated as the circuits works on resonance mode, the solution can be simplified as:

$$\begin{cases} \dot{i}_{ex} = \frac{u_{ex}}{r_{ex} + \sum \frac{\omega_0^2 M_{rei}^2}{r_{rei}}} \\ \dot{i}_{rei} = \frac{-j\omega_0 M_{rei}}{r_{rei}}\dot{i}_{ex} \end{cases}. \tag{8}$$

From (8), the total equivalent impedance R_{se} and individual equivalent impedance R_{reie} can be calculated as:

$$R_{se} = \sum \frac{\omega^2 M_{rei}^2}{r_{rei}} \tag{9}$$

$$R_{reie} = \frac{\omega^2 M_{rei}}{r_{rei}}. \tag{10}$$

As shown in (9), the equivalent impedance is connected in series in the excitation circuit. As shown in (10), equivalent impedance can be increased or decreased by reducing or enlarging r_{rei}.

According to (6), the multi-receptor charging system is equivalent to the circuit that is shown in Figure 1a, both excitation circuit and receptor works in resonance mode, namely the reactive impedance equals zero. According to (8), the circuit in Figure 1a can be furtherly simplified to the circuit in Figure 1b in which the equivalent impedance of different loads are connected in series.

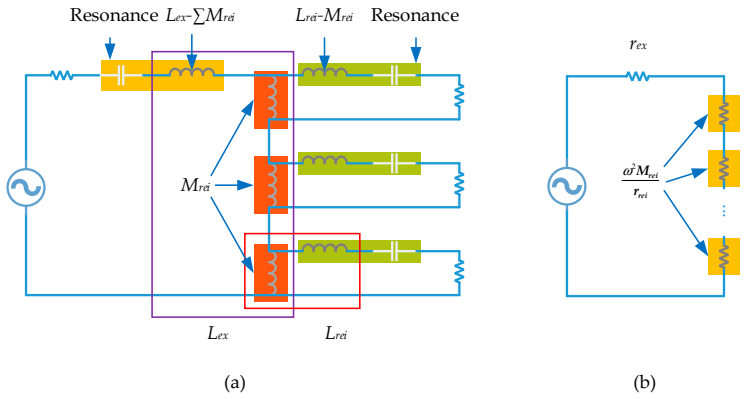

Figure 1. Equivalent circuit of multi-receptor charging system. (**a**) Inductance equivalent circuit; (**b**) Impedance equivalent circuit.

The output power P_{ex}, efficiency e and individual load power P_{rei} can be given by:

$$P_{ex} = \frac{1}{2}\frac{U_{ex}^2}{r_{ex} + R_{se}} \tag{11}$$

$$e = \frac{R_{se}}{r_{ex} + R_{se}} \tag{12}$$

$$P_{rei} = \frac{1}{2} I_{ex}^2 \frac{\omega_0^2 M_{rei}}{r_{rei}}, \tag{13}$$

where I_{ex} mean the amplitude of the excitation current and U_{ex} means the amplitude of the excitation voltage. The relationship between R_{se}, P_{ex}, e and P_{rei} is depicted in Figure 2. As shown in Figure 2, when R_{se} equals r_{ex}, P_{rei} can reach its maximum value and the efficiency is 50%. When R_{se} is larger than r_{ex}, P_{rei} decreases as the increment of R_{se}. Besides, the larger R_{se} is, the higher efficiency is.

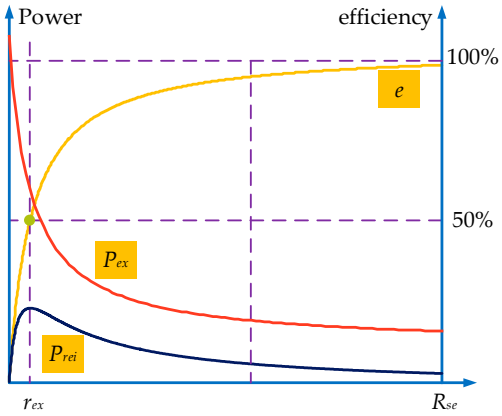

Figure 2. Relationship between R_{se}, P_{ex}, e and P_{rei}.

3. Load Adjustment and Power Distribution

3.1. Analysis of Power Distribution

In public application, the receptor is not identical. Besides, the number of load and individual load impedance are both random and vary unpredictably. As shown in Figure 1b, equivalent impedance of a different load is connected in the series in an equivalent circuit. As a result, the individual load with a larger equivalent impedance will be able to attain a larger portion of total power supply, and vice versa. Power of the *i*th load can be calculated as:

$$P_{rei} = \frac{1}{2} I_{ex}^2 \cdot R_{reie}. \tag{14}$$

For the individual load, once the power supply is deficient, the larger equivalent impedance ensures a larger portion of total power, while a smaller equivalent impedance will lead to a smaller portion of total power supply. Thus, the best and simplest strategy for individual load whose power is deficient is to enlarge its equivalent impedance. In the case of power surplus, the smaller equivalent impedance leads to a smaller portion of total power supply, while the larger equivalent impedance will lead to a larger portion of total power supply. As a result, the best and simplest strategy for individual load whose power is surplus is to reduce its equivalent impedance.

The *i*th Load power after adjustment is given by:

$$P_{rei} = \frac{1}{2}\left(\frac{U_{ex}}{r_{ex} + \sum(R_{reie} + \Delta R_{reie})}\right)^2 (R_{reie} + \Delta R_{reie}), \tag{15}$$

where ΔR_{reie} represents the increment of R_{reie} after adjustment. Power of total equivalent impedance P_t can be calculated by:

$$P_t = \frac{1}{2}\frac{U_{ex}^2}{r_{ex} + \sum(R_{reie} + \Delta R_{reie})}\left(\sum(R_{reie} + \Delta R_{reie})\right). \tag{16}$$

There is a special case that the sum of ΔR_{reie} equals 0. In this case, P_t equals total power demand and remains constant, the value of R_{se} in this case is the optimal value and remains constant. The adjustment of individual equivalent impedance R_{reie} is equivalent to adjust the equivalent impedance portion of a different load.

When P_t is lower than total power demand, adjusting a portion of individual equivalent impedance R_{reie} cannot achieve the optimal power distribution, namely, not all power demand will be satisfied. Some loads whose power is lower than demand will enlarge their equivalent impedance to acquire a larger portion of total power supply, which will cause some other loads to obtain deficient power and start enlarging their equivalent impedance. Therefore, more and more loads enlarge their impedance. As analyzed in Section 2, the larger total equivalent impedance is, the lower power all loads will share. Finally, all loads enlarge their equivalent impedance to the maximum value and the current of the excitation circuit meet its minimum value.

In the case of power surplus, adjusting a portion of individual equivalent impedance R_{reie} cannot satisfy all power demand either. In this case, some loads whose power is higher than demand will reduce their equivalent impedance to obtain a smaller portion of total power supply, which will cause some other loads to obtain surplus power and start reducing their equivalent impedance. Therefore, more and more loads reduce their equivalent impedance. The smaller total equivalent impedance is, the higher power all loads will share. Finally, all loads reduce their equivalent impedance to the minimum value and the current of the excitation circuit meet its maximum value.

According to the above analysis, optimal power distribution need not only the adjustment of individual equivalent impedance, but also the adjustment of total equivalent impedance. And only when total power supply satisfies load power demand, will the balance be achieved. In this case, loads whose power is higher than power demand will reduce their impedance and other loads whose power is lower than power demand will enlarge their impedance. When all load power demand is satisfied, load impedance adjustment stops and the appropriate power distribution is achieved.

In the case that the charging object is moving such as EV, the effect of mutual inductance should be taken into consideration. As deduced from (10), the smaller load impedance r_{rei} is, the larger equivalent impedance r_{eie} is, the larger mutual inductance M_{rei} is, and the larger equivalent impedance is. Actually, there exists a minimum value of r_{rei}, the maximum equivalent impedance can be calculated as:

$$r_{reiemax} = \frac{\omega^2 M_{rei}^2}{r_{reimin}}, \tag{17}$$

where r_{reimin} means the minimum value of load impedance r_{rei}, and r_{reimax} means the maximum value of equivalent impedance r_{reie}. There is also a maximum amplitude of the excitation current I_{ex}. If load impedance meets its minimum value r_{reimin} and I_{ex} meets its maximum value, the power of the individual load depends on the mutual inductance. And only when the mutual inductance is large enough, individual load can enlarge its equivalent impedance and make the excitation circuit reduce total equivalent impedance. As a result, the power demand cannot be satisfied in the case that mutual inductance is too small.

In the case of charging batteries and super capacitors, the power demand is not constant and varies as the state of charge changes. Therefore, optimal power distribution should be achieved dynamically with fast response and high stability.

Practically, the speed of equivalent impedance adjustment of a different load is not identical, which causes the sum of the increment of the individual load equivalent impedance ΔR_{reie} unequal to 0. According to the analysis of Section 2, once the total equivalent impedance is larger or smaller than the optimal value of R_{se}, the power of the total equivalent impedance is lower or higher than

total power demand, which will furtherly cause the total equivalent impedance to increase or decrease sharply. In this case, even the total equivalent impedance R_{se} equals the optimal value, the appropriate power distribution cannot be achieved. To ensure the robustness of the system, the power of total equivalent impedance P_t should be able to endure the fluctuation. As long as the power of total equivalent impedance P_t remains constant, the optimal power distribution will finally be achieved.

3.2. Principle of Load Adjustment

An efficient way to adjust individual load is to use a rectifier and a DC-DC converter to change the equivalent impedance by adjusting its duty ratio. The relation between the input and the output impedance in Cuk circuit is given by:

$$r_{rei} = \left(\frac{1-\alpha}{\alpha}\right)^2 R_{Li}, \tag{18}$$

where α means the duty ratio of Cuk circuit, R_{li} represents the real load impedance. According to the power of the ith load, input voltage of the DC-DC converter u_{rei} can be calculated as:

$$U_{rei} = \frac{1-\alpha}{\alpha}\sqrt{P_{rei}R_{Li}}, \tag{19}$$

where U_{rei} means the DC input voltage of the DC-DC converter. According to the input voltage of the DC-DC converter of the ith load u_{rei} and the power demand of the ith load P_{refi}, the duty ratio α can be calculated as:

$$\alpha = \frac{\sqrt{P_{refi}R_{Li}}}{U_{rei} + \sqrt{P_{reif}R_{Li}}}. \tag{20}$$

In Reference [23], a total equivalent impedance adjusting method was proposed, a capacitor C_p is connected in parallel with the excitation current. The total equivalent impedance can be adjusted by changing the capacitor C_p. the total equivalent impedance can be adjusted to:

$$R'_{se} = \frac{R_{se}}{1 - 2\omega_0^2 C_p L_{ex} + \omega_0^2 C_p^2 R_{se}^2 + \omega_0^4 C_p^2 L_{ex}^2}. \tag{21}$$

The relationship between capacitance of C_p, total equivalent impedance R_{se}, output power P_{ex} and efficiency e is depicted in Figure 3. As shown in Figure 3, the total equivalent impedance can be adjusted between the maximum value and the minimum value by selecting the appropriate value of C_p. Besides, the larger total equivalent is, the higher the efficiency is.

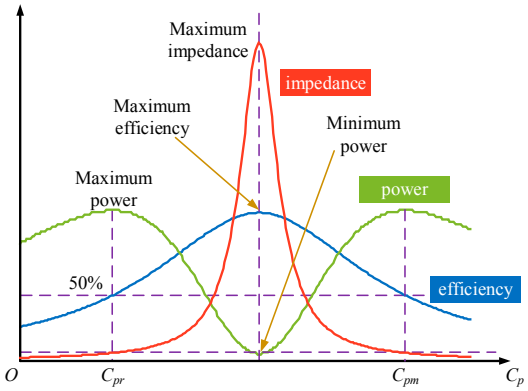

Figure 3. Relationship among equivalent impedance, power efficiency and C_p.

The circuit of the multi-objective WPT system is shown in Figure 4. Each receptor has an impedance regulator to adjust the equivalent impedance, aiming to meet various demands of the load power. The equivalent impedance of each load is adjusted according to the obtained power by the receptors. In the excitation circuit, a current sensor is used to detect load variation and the controller alters the capacitor array C_p to alter the total equivalent impedance. A smart injection circuit is used to inject a current to compensate the voltage of C_{ex} to match the reactive impedance of excitation circuit to ensure the circuit works in resonant mode. A couple of capacitors and inductors are used at the input port of the inverter to ensure power fluctuation tolerance.

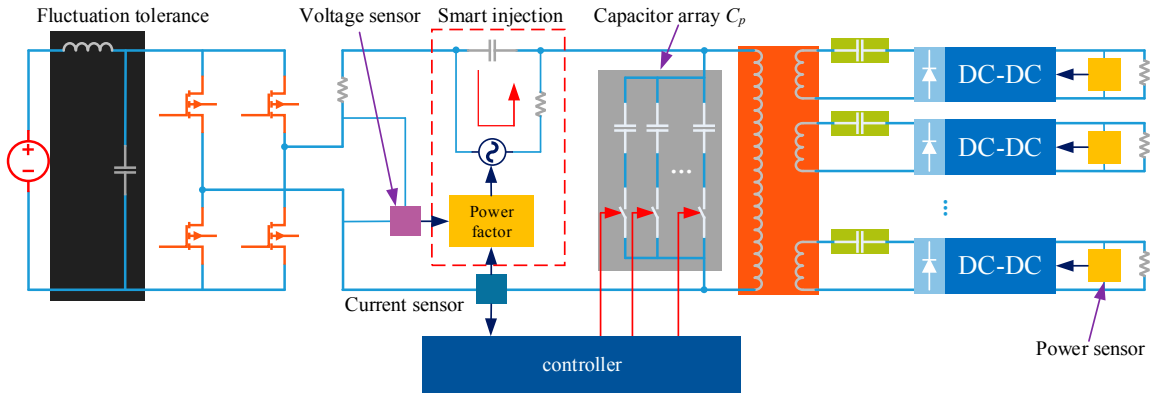

Figure 4. Equivalent circuit.

3.3. Methodology of Load Adjustment

As analyzed in Section 3.1, only when the total equivalent impedance equals the optimal value, can the appropriate power distribution be achieved. If the total equivalent impedance is larger than the optimal value, the total equivalent impedance will increase sharply. While if the total impedance is smaller than the optimal value, total equivalent impedance will decrease sharply. An optimal power distribution control method was proposed according to the analysis in Section 3.1.

The main idea of the control method is to find the optimal value of the total equivalent impedance. The variation of the excitation current, which reflects the variation total equivalent impedance caused by individual load adjustment, can be used as the indicator of total equivalent impedance adjustment. When the optimal value of the total equivalent impedance is found, the total equivalent impedance remains constant, after the adjustment of the power portion of the different load, appropriate power distribution is achieved. The optimal total equivalent impedance is solved by the dichotomy. Namely, find the medium value between the maximum value and the minimum value, and set the current value as the minimum value when the optimal value is larger than the current value or set the current value as the maximum value when the optimal value is smaller than the current value. The variation of I_{ex} reflects whether the optimal total equivalent impedance is larger or smaller than the current total equivalent impedance. The time complexity of the solving process is given by the following equation:

$$\Theta(t) = \log_2 N - 1, \tag{22}$$

where N represents the number of the available value of capacitor C_p. From formula (22), the time cost is greatly reduced and thus the speed of response is greatly improved.

Figure 5 portraits the procedure of impedance adjustment. The case of power surplus is shown in Figure 5a, and the case of power deficiency is depicted in Figure 5b. As shown in Figure 5a, in the first step, all loads reduce their equivalent impedance and their power is much higher than their demand. In the second step, the controller alters the total equivalent impedance to the medium value between the maximum value and the minimum value and the total equivalent impedance in step 1 is set as the minimum value, and load power decreases correspondingly. After the adjustment

of step 2, total equivalent impedance is still smaller than the optimal value. In the third step, the individual loads reduce their equivalent impedance for a smaller portion of total power, and the total equivalent impedance decreases sharply. According to the variation of the total equivalent impedance, the controller altered the total equivalent impedance to the medium value between the maximum value and the minimum value in the fourth step. At this time, total equivalent impedance is close to the optimal total equivalent impedance. In the fifth step, a different load with a different power demand alters their equivalent impedance to achieve the appropriate power distribution.

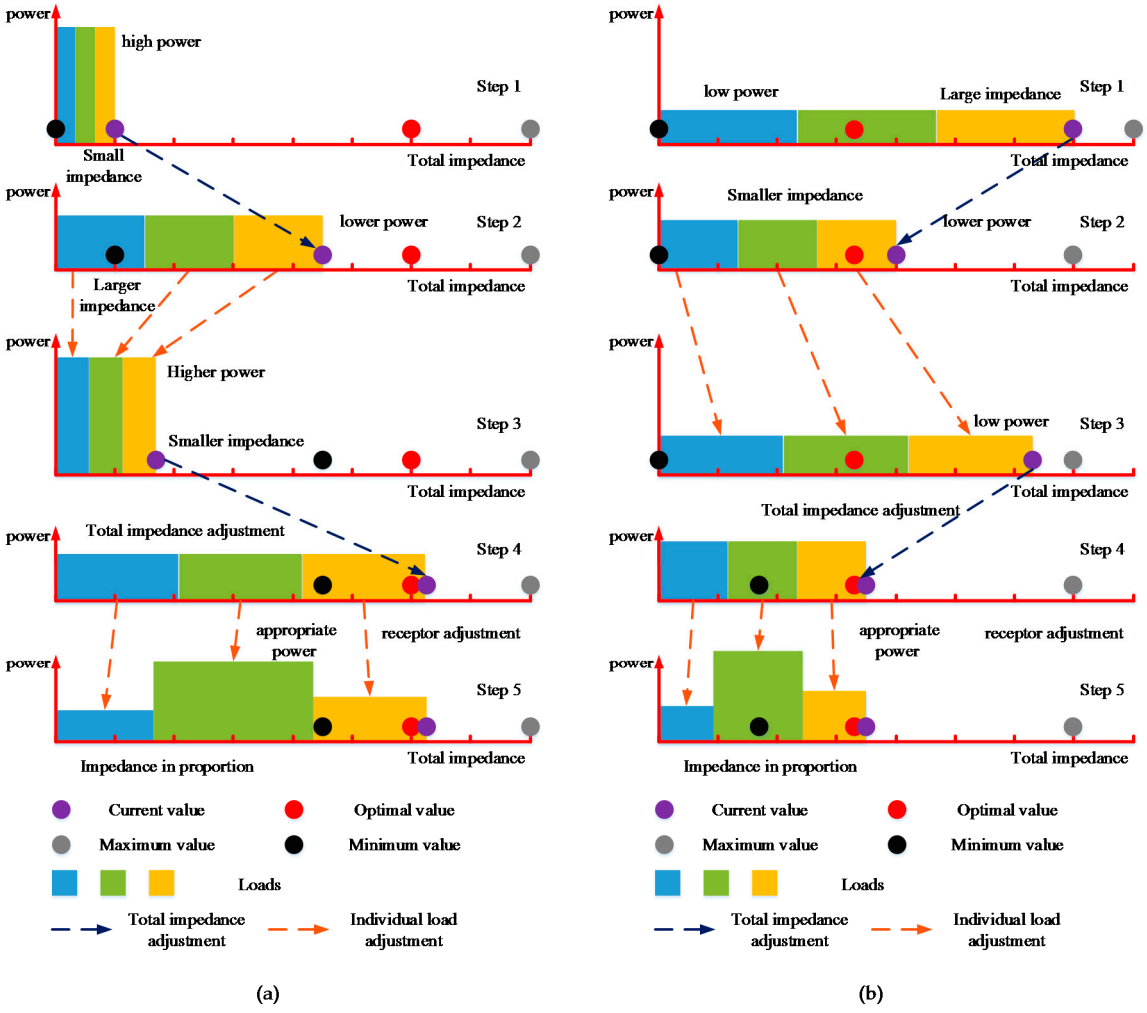

Figure 5. Load adjustment process. (**a**) power surplus case, (**b**) power deficiency case.

The adjustment procedure in the case of power deficiency is depicted in Figure 5b. In the first step, due to power deficiency, all loads enlarge their equivalent impedance to the maximum value. In the second step, the controller reduces the total equivalent impedance to the medium value between the maximum value and the minimum value, and the total equivalent impedance in step 1 is set as the maximum value, and load power increases correspondingly. Due to the total equivalent impedance still being larger than the optimal value, individual loads enlarge their equivalent impedance for a larger power portion in the third step. In the fourth step, total equivalent impedance is altered to the medium value between the maximum and the minimum value, at this time, total equivalent impedance is close to the optimal value. In the fifth step, a different load with a different power demand adjusts their equivalent impedance to achieve the appropriate power distribution.

The pseudo code of the total equivalent impedance adjustment is shown in Algorithm 1.

Algorithm 1

Initialize(R_{exmax}, R_{exmin}, i_{exmax})
while(ture) **do** // find the optimal value by dichotomy.
  input(I_{ex}) // use the excitation current to detect total equivalent impedance variation.
  if($I_{ex} > I_{exmax}$)
    break // if there is no charging load or the charging load is to heavy, close the system.
  end if
  if $I_{ex} > 1.5 \times I_{ex0}$ // total equivalent impedance decreases sharply.
    $R_{se} \leftarrow U_{ex}/I_{ex} - r_{ex}$
    $R'_{se} \leftarrow (R_{exmax} + R_{exmin})/2$ // set the total equivalent impedance to the medium value.
    $R_{exmin} \leftarrow R_{se}$ // set the current value as the minimum value.
    $C_p \leftarrow \frac{2\omega_0^2 R'_{se} L_{ex} + \sqrt{4\omega_0^2 R'^2_{se} L^2_{ex} - 4R'_{se}\left(\omega_0^2 R^2_{se} + \omega_0^2 L_{ex}\right)(R'_{se} - R_{se})}}{2R'_{se}\left(\omega_0^2 R^2_{se} + \omega_0^4 L^2_{ex}\right)}$
    input(I_{ex})
    $I_{ex0} \leftarrow I_{ex}$ // record the excitation current to detect if total equivalent impedance changes.
  else if $I_{ex} < 0.066 \times I_{ex0}$ // total equivalent impedance increases sharply.
    $R_{se} \leftarrow U_{ex}/I_{ex} - r_{ex}$
    $R'_{se} \leftarrow (R_{exmax} + R_{exmin})/2$ // set the total equivalent impedance to the medium value.
    $R_{exmax} \leftarrow R_{se}$
    $C_p \leftarrow \frac{2\omega_0^2 R'_{se} L_{ex} + \sqrt{4\omega_0^2 R'^2_{se} L^2_{ex} - 4R'_{se}\left(\omega_0^2 R^2_{se} + \omega_0^2 L_{ex}\right)(R'_{se} - R_{se})}}{2R'_{se}\left(\omega_0^2 R^2_{se} + \omega_0^4 L^2_{ex}\right)}$
    input(I_{ex})
    $I_{ex0} \leftarrow I_{ex}$ // record the excitation current to detect if total equivalent impedance changes.
  end if
  if t%50 = 0
    Initialize(R_{exmax}, R_{exmin}) //every 50 steps reinitialize R_{exmax} and R_{exmin}.
  end if
  t$\leftarrow$t + 0.001 //each step cost 1 ms.
end

The pseudo code of the individual equivalent impedance adjustment is shown in Algorithm 2.

Algorithm 2

Initialize(α, P_{refi})
while(true) **do**
  input(P_{rei})
$U_{rei} \leftarrow \frac{1-\alpha}{\alpha}\sqrt{P_{rei} R_{Li}}$ // calculate input voltage of the DC-DC converter.
  if $P_{rei} \neq P_{refi}$
    $\alpha \leftarrow \frac{\sqrt{P_{refi} R_{Li}}}{U_{rei} + \sqrt{P_{refi} R_{Li}}}$ // if the power demand is not satisfied, adjust the duty ratio.
  end if
  t$\leftarrow$t + 0.003 // each step cost 3 ms.
end

4. Verification

4.1. Simulated Results

To verify the validity of the proposed scheme, a computational simulation is carried out by using three receptors. In order to further demonstrate the feasibility, stability, accuracy and response speed of the proposed power distribution scheme in different cases, four case studies are given in this paper, including Case 1 to verify the effectiveness of the proposed scheme; Case 2 to illustrate the multi-channel transmission performance by taking into account the variation of power demand;

Case 3 to verify the response speed, accuracy and stability for charging moving EVs and Case 4 to demonstrate the effectiveness of the proposed scheme for charging batteries and super capacitors. Key parameters are listed in Table 1.

Table 1. Key parameters.

Parameter	Symbol	Value
Real impedance of Load 1	$R1$	100 Ω
Real impedance of Load 2	$R2$	100 Ω
Real impedance of Load 3	$R3$	100 Ω
Demand power range of Load 1	P_{r1}	18–40 W
Demand power range of Load 2	P_{r2}	35–45 W
Demand power range of Load 3	P_{r3}	27–40 W
Power demand range of EV 1	P_{Er1}	4500–5500 W
Power demand range of EV 2	P_{Er2}	2700–3300 W
Power demand range of EV 3	P_{Er3}	1800–2200 W
Power error tolerance	e_P	10%
Excitation coil inductance	L_{ex}	1 mH
Receptor inductance	L_{re}	400 μH
Power supply voltage	u_{ex}	200 V
Working frequency	f	20 kHz

Case 1—The comparative simulation is firstly carried out for charging potable electronics as shown in Figure 6. During t = 0~3 s, the impedance regulators of the excitation circuit and receptor circuit are inactivated. In such a case, the power of Load 1, Load 2 and Load 3 equal 32.7 W, which causes power deficiency of load 2. At t = 3 s, the impedance regulator of receptor 1 and receptor 2 are activated while the impedance regulator of receptor 3 remains inactive. The power deficiency of Load 2 results in the increasing of the equivalent impedance of Load 2, thus leading to the power deficiency of Load 1 and Load 3. Due to the increased equivalent impedances of Load 1 and Load 2, the total supply power reduces to 8.8 W, while Load 1 and Load 2 obtain a larger portion of power supply. At t = 7 s, when the impedance regulator of excitation circuit is activated, the total equivalent impedance is adjusted to satisfy the power demand of loads. The power of Load 1 and Load 2 can meet the minimum demand, namely P_{re1} = 21.7 W and P_{re2} = 42.3 W, by adopting the proposed control scheme; while the impedance regulator is inactivated, the power of Load 3 (64.8 W) exceeds the maximum power demand (40 W). Thus, the proposed control scheme can effectively ensure the load power demand.

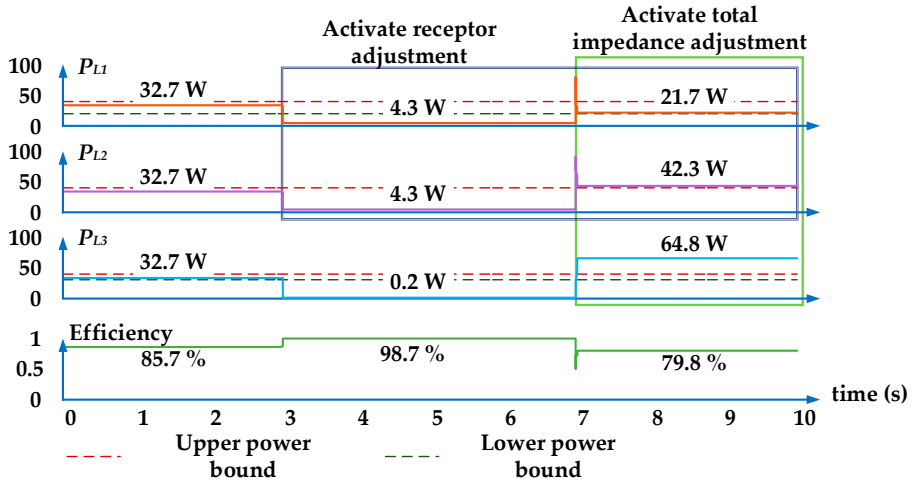

Figure 6. Comparative results.

Case 2—By adding and removing loads, a test is carried out by taking into account the variation of power demand in charging portable electronics, which aims to further illustrate the effectiveness of the proposed control scheme. All impedance regulators are activated through the whole testing process. The charging procedure is depicted in Figures 7 and 8.

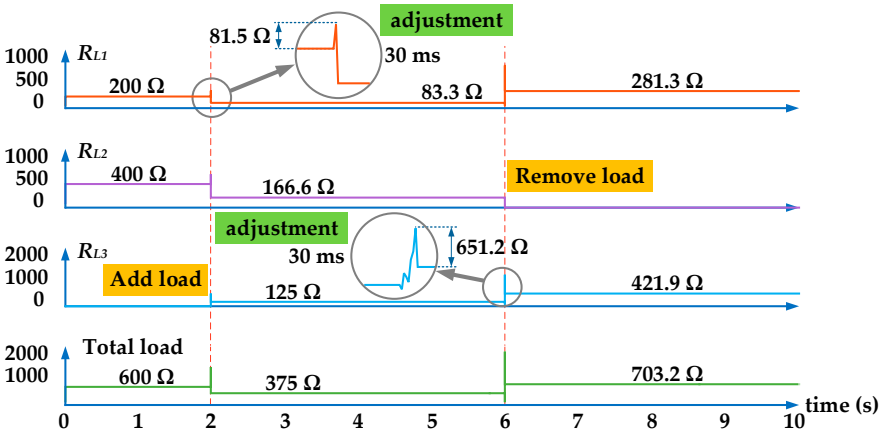

Figure 7. Power and efficiency.

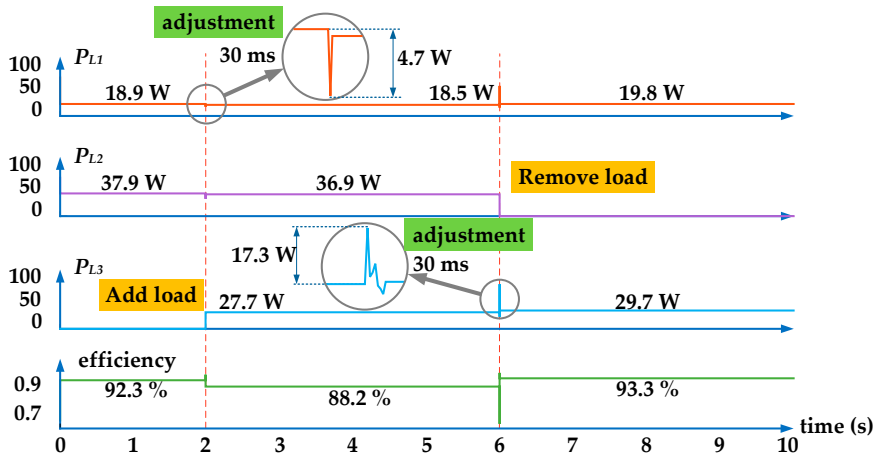

Figure 8. Equivalent impedance.

As shown in Figure 7, Load 1 and Load 2 are in the charging state during t = 0~2 s, where R_{re1e} = 200 Ω, R_{re2e} = 400 Ω, R_{re3e} = 0 Ω, and P_{re1} = 18.9 W, P_{re2} = 37.9 W and P_{re3} = 0 W. At t = 2 s, Load 3 is added, which results in an immediate power deficiency of all loads as shown in Figure 8, power deficiency incurs larger impedance as shown in Figure 7. By adjusting the total impedance equaling 375 Ω, the load power meets the minimum demand, namely P_{re1} = 18.5 W, P_{re2} = 36.9 W, and P_{re3} = 27.7 W. At t = 6 s, Load 2 is removed, which causes an immediate power surplus. The total impedance is adjusted to 703.2 Ω. The impedance and power of loads remain R_{re1e} = 281.3 Ω, R_{re2e} = 0 Ω, R_{re3e} = 421.9 Ω, P_{re1} = 19.8 W, P_{re2} = 0 W and P_{re3} = 27.9 W. Then, as shown in Figure 8, the loads power meets the demand again. Based on the relationship as shown in Figure 2, the proposed control scheme can ensure the power supply meets the minimum power demand, which means the multi-objective WPT system can work at the maximum efficiency point even if there is a variation of power demand.

Case 3—The charging demand of the moving objects is also taken into consideration to further verify the validity and effectiveness of the proposed method. Figure 9 portraits the charging procedure of moving EVs. There are in total, three EVs passed by. As shown in Figure 9a. At t = 1 s, EV 3

moved into the charging area, during t = 1~2.5 s, power of EV 3 increased as EV 3 was approaching the excitation coil. During t = 2.5~4 s, power demand of EV 3 was satisfied and the power of EV 3 was kept stable at 1921 W. At t = 4 s, EV 2 which has a higher speed and higher power demand moved into the charging area, which caused an immediate change of total power demand and total equivalent impedance. After the adjustment, the power of EV 3 was kept stable at 2148 W. During t = 4~5 s power of EV 2 increased as EV 2 approached the excitation coil. At t = 4.5 s, the power of EV 3 started decreasing due to the decrement of mutual inductance and EV 1 moved into the charging area. Due to the higher speed and higher power demand of EV 1, total power demand and total equivalent impedance varied at a higher speed, which caused the overshoot of the adjustment to be much larger, and EV 1 and EV 2 obtained the maximum power of P_{re1} = 6797 W and P_{re2} = 5215 W. At t = 5 s, the power of EV 1 and EV 2 met the power demand and were kept stable at P_{re1} = 4786 W and P_{re2} = 2874 W. At t = 6 s, the power of EV 1 and EV 2 started decreasing. After t = 7.3 s, there was no EV to charge and the total power was kept to zero.

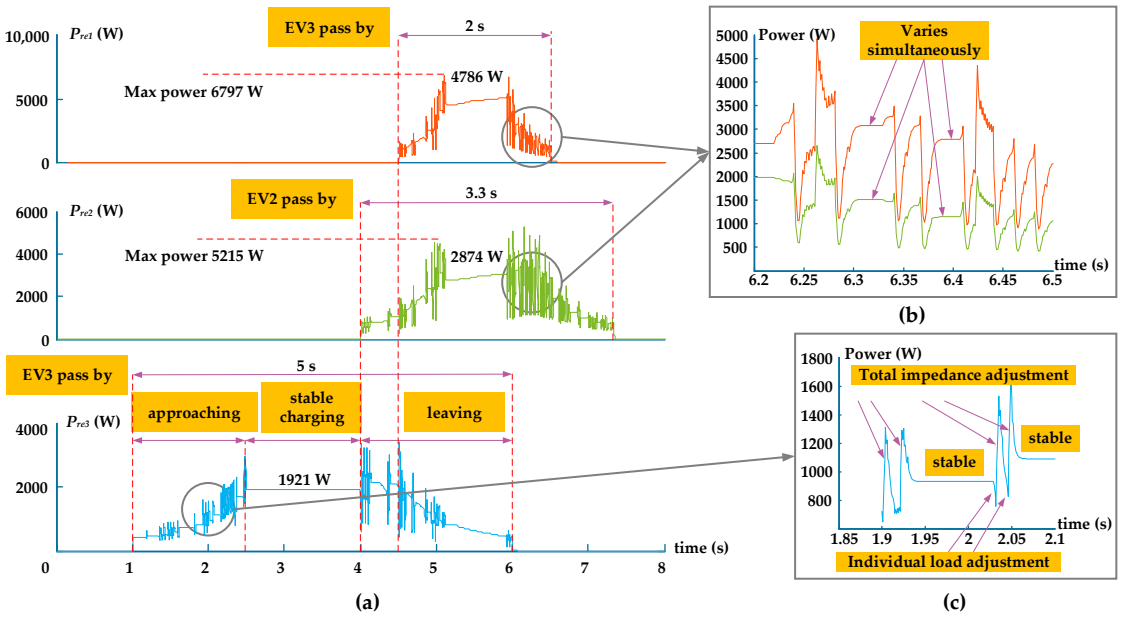

Figure 9. EV charging procedure. (**a**) Whole charging procedure. (**b**) Detailed charging procedure of power fluctuation. (**c**) Detailed procedure in power demand variation.

The detailed charging procedure in the case of power fluctuation is depicted in Figure 9b. During t = 6.2~6.5 s, EV 1 and EV 2 cannot obtain enough power. Thus they dynamically adjust their equivalent impedance for a larger power portion. Due to the adjustment of EV 1, EV 2 and the excitation circuit, power of EV 1 and EV 2 fluxed in a limited range and continued decreasing, which proved the rapidity and stability of the proposed method.

The charging detail of EV 1 in the case of power variation is shown in Figure 9c. During t = 1.85~2.1 s, power demand of EV 1 was not satisfied. During t = 1.9~2.05 s, as the mutual inductance increased, the equivalent impedance increased at t = 2.03 s, which caused a power decrease, and the excitation circuit altered the total equivalent impedance to a smaller value and the power increased. At t = 2.07 s, the power of the load kept stable but did not satisfy the power demand due to the limitation of mutual inductance.

According to the charging procedure depicted in Figure 9, the ability for charging moving objects with high speed and high power demand is well proved. Namely, the proposed method can charge multiple moving EVs dynamically with fast response and high stability.

Case 4—The case of power demand variation is also considered and simulated. The charging procedure of batteries and super capacitors is depicted in Figure 10, it depicts the procedure of charging

batteries and super capacitors, respectively. As shown in Figure 10a, at t = 0.5 h, battery 1 started charging and charged in trickle mode, the charging power P_{re1} equaled 1441 W and was kept constant. At t = 1.2 h, battery 1 shifted into constant current mode, and the charging power demand increased to 7044 W. At t = 1.5 h, battery 2 started charging in trickle mode with P_{re2} = 1961 W, the sudden change of power demand and equivalent impedance caused a power fluctuation with the maximum overshoot of 0.76 on battery 1. At t = 1.9 h, battery 2 shifted to constant current mode and kept the charging power to 11047 W. At t = 2.2 h, battery 1 shifted to constant voltage mode and power demand started decreasing continuously. At t = 2.5 h, battery 2 shifted to constant voltage mode and power started decreasing continuously. Total demanded energy and charged energy of battery 1 and battery 2 equaled 36 GJ, 36.42 GJ, 29.77 GJ and 28.62 GJ, respectively, which implies that the energy accuracy is in the range of 95~105%.

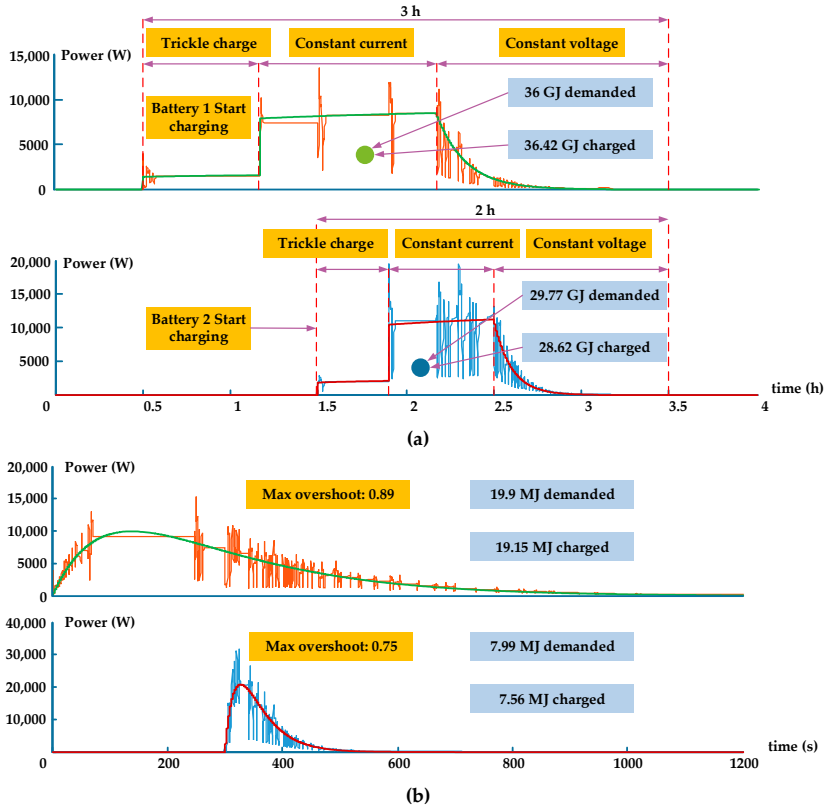

Figure 10. Charging procedure of batteries and super capacitors. (**a**) Charging procedure of batteries. (**b**) Charging procedure of super capacitors.

Figure 10b depicts the charging procedure of two super capacitors. Power demand varies continuously. Maximum overshoot of super capacitor 1 and super capacitor 2 equals 0.89 and 0.75 respectively. Total demanded energy and charged energy of super capacitor 1 and super capacitor 2 equals 19.9 MJ, 19.15 MJ, 7.99 MJ and 7.56 MJ, respectively. The energy accuracy is in the range of 95–105%.

The simulation well proved that the proposed control method can achieve optimal power distribution with fast response, high accuracy and high stability.

4.2. Experimental Results

In order to further demonstrate the validity of the proposed scheme, an experimental prototype was carried out as shown in Figure 11, where the demand power range of Load 1 and Load 2 were set as 1.5~2.5 W and 3~4 W, respectively.

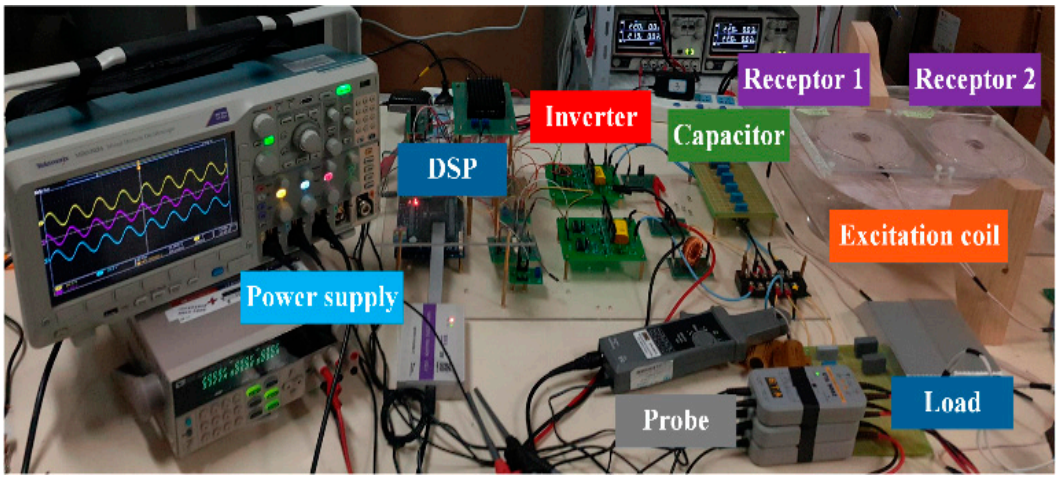

Figure 11. Experimental prototype.

As shown in Figure 12a, the procedure stated in power surplus condition, each load adjusted their equivalent impedance to its minimum value, namely R_{e1} = 2.4 Ω and R_{e2} = 3.7 Ω. The voltages of Load 1 and Load 2 are 8 V and 9 V, respectively. The power of Load 1 and Load 2 reached the maximum value, namely 4.3 W and 5.4 W. Due to the sharp increment of the excitation current, the capacitor C_p is adjusted to 47 nF, aiming to reducing the load power immediately. As shown in Figure 12b, due to the adjustment of the total equivalent impedance, the voltage and the power of Load 1 and Load 2 decrease to 4.9 V, 5.1 V, 1.6 W and 1.7 W, respectively, load power demand is not satisfied. In the case of power deficiency, the proposed impedance regulator increases the equivalent impedance of Load 1 and Load 2 to 7.2 Ω and 11 Ω for a larger portion of total power supply, the excitation current decreases correspondingly. As shown in Figure 12c, the voltage of each load decreases to 2.6 V and 2.2 V. Additionally, the load power reduces to the minimal values, namely 1.3 W and 1 W. Since total impedance increases sharply, namely the excitation current increases sharply, the capacitor array C_p changes the capacitance to 16.8 nF. The optimal value of the total equivalent impedance is found and total supply power increases and matches the power demand. As shown in Figure 12d, the impedance of Load 1 and Load 2 are adjusted in the proportion of the power demand. Accordingly, the power of Load 1 and Load 2 meet the demand, namely 2 W and 3 W. Optimal power distribution is achieved through a four-step adjustment. At this time, the output power of DC power supply is 6.64 W. Total efficiency of the charging system is 75.3%. Thus, the experimental results well agree with the theoretical analysis and simulated results, which has verified that the proposed scheme can ensure the optimal power distribution for multi-objective WPT systems with fast response, high stability and high accuracy.

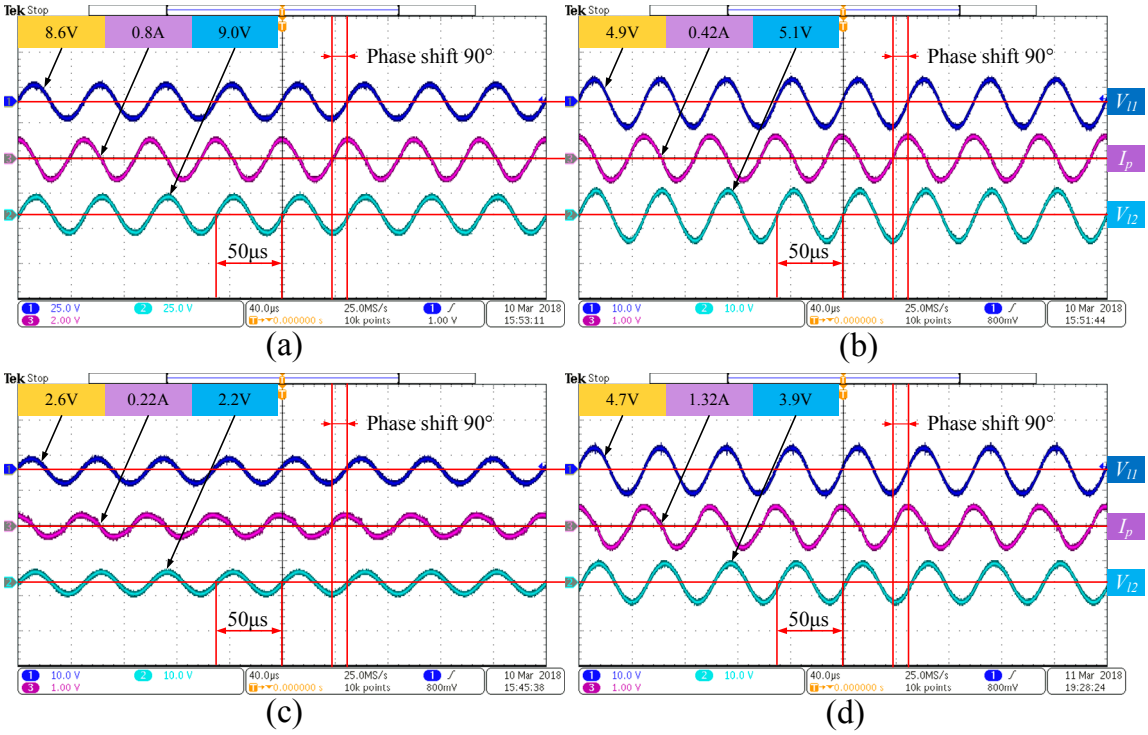

Figure 12. Measured waveforms with Ch1: Load 1 voltage (25 V/div in (**a**) and 10 V/div in (**b**–**d**), Ch2: Load 2 voltage (25 V/div in (**a**) and 10 V/div in (**b**–**d**), Ch3: primary circuit current (2 A/div in (**a**) and 1 A/div in (**b**–**d**), (40µs/div): (**a**) R_{l1} = 15 Ω, R_{l2} = 15 Ω and C_p = 0 nF; (**b**) R_{l1} = 15 Ω, R_{l2} = 15 Ω and C_p = 47 nF; (**c**) R_{l1} = 5 Ω, R_{l2} = 5 Ω and C_p = 47 nF; (**d**) R_{l1} = 10 Ω, R_{l2} = 5 Ω and C_p = 16.8 nF.

5. Conclusions

This paper proposed an optimal power distribution scheme for multi-objective WPT systems, which can effectively satisfy various power demands from multiple loads without any communication networks. By adopting the DC/DC-converter-based load impedance adjustment and the capacitor-array-based total impedance adjustment schemes, the proposed power distribution scheme can successfully satisfy different power demands for multiple loads with fast response, high stability and high accuracy. Thus, this can be used for charging portable electronics, implantable devices and EVs. The corresponding simulated and experimental results well agree with the theoretical analysis, which has illustrated the enhanced transmission performance for multi-objective WPT systems.

Author Contributions: Conceptualization, Z.Z. and R.T.; Methodology, R.T.; Validation, R.T.; Formal Analysis, R.T. and Z.L.; Writing-Original Draft Preparation, R.T.; Writing-Review & Editing, Z.L. and C.L.; Supervision, Z.Z. and J.W.; Project Administration, J.W.; Funding Acquisition, Z.Z.

Acknowledgments: This work was supported in part by the National Natural Science Foundation of China under Project 51607120, in part by the Natural Science Foundation of Tianjin China under Project 16JCQNJC01500, and in part by the Tianjin University, Tianjin, China, PEIYANG Scholar-Reserved Academic Program under Project 2017XRX-0017.

Conflicts of Interest: The authors declare no conflict of interest.

References

1. Wang, C.S.; Grant, C.A.; Stielau, O.H. Power transfer capability and bifurcation phenomena of loosely coupled inductive power transfer systems. *IEEE Trans. Ind. Electron.* **2004**, *51*, 148–157. [CrossRef]
2. Liu, X.; Hui, S.Y. Optimal design of a hybrid winding structure for planar contactless battery charging platform. *IEEE Trans. Power Electron.* **2008**, *23*, 455–463.

3. Low, Z.N.; Chinga, R.A.; Tseng, R.; Lin, J. Design and test of a high-power high-efficiency loosely coupled planar wireless power transfer system. *IEEE Trans. Ind. Electron.* **2009**, *56*, 1801–1812.
4. Jiang, C.; Chau, K.T.; Liu, C.; Lee, H.T.C. An overview of resonant circuits for wireless power transfer. *Energies* **2017**, *8*, 894. [CrossRef]
5. Jang, Y.; Jovanović, M.M. A contactless electrical energy transmission system for portable-telephone battery chargers. *IEEE Trans. Ind. Electron.* **2003**, *50*, 520–527. [CrossRef]
6. Chau, K.T.; Chan, C.C.; Liu, C. Overview of permanent-magnet brushless drives for electric and hybrid electric vehicles. *IEEE Trans. Ind. Electron.* **2008**, *55*, 2246–2257. [CrossRef]
7. Lu, Y.; Brain, M.D. Wireless power transfer system architecture for portable or implantable applications. *Energies* **2016**, *9*, 1087. [CrossRef]
8. Chau, K.T.; Chan, C.C. Emerging energy-efficient technologies for hybrid electric vehicles. *IEEE Proc.* **2007**, *95*, 821–835. [CrossRef]
9. Rao, S.; Chiao, J.C. Body electric wireless power transfer for implant applications. *IEEE Microw. Mag.* **2015**, *16*, 54–64. [CrossRef]
10. Lee, H.T.C.; Chau, K.T.; Liu, C. Design and Analysis of an Electronic-Geared Magnetless Machine for Electric Vehicles. *IEEE Trans. Ind. Electron.* **2016**, *63*, 6705–6714. [CrossRef]
11. Zhang, Z.; Chau, K.T. Pulse-Width-Modulation-Based electromagnetic interference mitigation of bidirectional grid-connected converters for electric vehicles. *IEEE Smart Grid* **2017**, *8*, 2803–2812. [CrossRef]
12. Giuseppe, B.; Manuele, B.; Kishore, N.M. Design and experimentation of WPT charger for electric city car. *IEEE Trans. Ind. Electron.* **2015**, *62*, 7436–7447.
13. Zhang, Z.; Chau, K.T. Homogeneous wireless power transfer for move and charge. *IEEE Trans. Power Electron.* **2015**, *30*, 6213–6220. [CrossRef]
14. Bu, Y.; Mizuno, T.; Fujisawa, H. Proposal of a wireless power transfer technique for low-power multi-receiver applications. *IEEE Trans. Magn.* **2015**, *51*, 1–4. [CrossRef]
15. Hatanaka, K.; Sato, F.; Matsuki, H.; Kikuchi, S.; Murakami, J.; Kawase, M.; Satoh, T. Power transmission of a desk with a cord-free power supply. *IEEE Trans. Magn.* **2002**, *38*, 3329–3331. [CrossRef]
16. Cheon, S.; Kim, Y.; Kang, S.; Lee, M.; Lee, J.; Zyung, T. Circuit-model-based analysis of a wireless energy-transfer system via coupled magnetic resonances. *IEEE Trans. Ind. Electron.* **2011**, *58*, 2906–2914. [CrossRef]
17. Kiani, M.; Ghovanloo, M. The circuit theory behind coupled-mode magnetic resonance-based wireless power transmission. *IEEE Trans. Circuits Syst. I Reg. Lett.* **2012**, *59*, 1–10. [CrossRef] [PubMed]
18. Imura, T.; Hori, Y. Maximizing air gap and efficiency of magnetic resonant coupling for wireless power transfer using equivalent circuit and Neumann formula. *IEEE Trans. Ind. Electron.* **2011**, *58*, 4746–4752. [CrossRef]
19. Dai, X.; Li, X.; Li, Y.; Deng, P.; Tang, C. A maximum power transfer tracking method for WPT systems with coupling coefficient identification considering two value problem. *Energies* **2017**, *10*, 1665. [CrossRef]
20. Zhang, Z.; Chau, K.T.; Liu, C.; Qiu, C.; Lin, F. An efficient wireless power transfer system with security considerations for electric vehicle applications. *J. Appl. Phys.* **2014**, *115*, 17A328. [CrossRef]
21. Zhang, Z.; Chau, K.T.; Qiu, C.; Liu, C. Energy encryption for wireless power transfer. *IEEE Trans. Power Electron.* **2015**, *30*, 5237–5246. [CrossRef]
22. Lee, K.; Cho, D. Analysis of wireless power transfer for adjustable power distribution among multiple receivers. *IEEE Trans. Power Electron.* **2015**, *14*, 950–953. [CrossRef]
23. Lim, Y.; Tang, H.; Lim, S.; Park, J. An adaptive impedance-matching network based on a novel capacitor matrix for wireless power transfer. *IEEE Trans. Power Electron.* **2014**, *29*, 4403–4413. [CrossRef]